

Review

Positron Emission Tomography Imaging of Atherosclerosis

Hakan Orbay¹, Hao Hong¹, Yin Zhang², Weibo Cai^{1,2,3}✉

1. Department of Radiology, University of Wisconsin - Madison, WI, USA;
2. Department of Medical Physics, University of Wisconsin - Madison, WI, USA;
3. University of Wisconsin Carbone Cancer Center, Madison, WI, USA.

✉ Corresponding author: Weibo Cai, PhD, Departments of Radiology and Medical Physics, School of Medicine and Public Health, University of Wisconsin - Madison, 1111 Highland Ave, Room 7137, Madison, WI 53705-2275, USA. Fax: 1-608-265-0614; Tel: 1-608-262-1749; Email: wcai@uwhealth.org.

© Ivyspring International Publisher. This is an open-access article distributed under the terms of the Creative Commons License (<http://creativecommons.org/licenses/by-nc-nd/3.0/>). Reproduction is permitted for personal, noncommercial use, provided that the article is in whole, unmodified, and properly cited.

Received: 2012.11.08; Accepted: 2013.01.27; Published: 2013.11.02

Abstract

Atherosclerosis-related cardiovascular events are the leading causes of death in the industrialized world. Atherosclerosis develops insidiously and the initial manifestation is usually sudden cardiac death, stroke, or myocardial infarction. Molecular imaging is a valuable tool to identify the disease at an early stage before fatal manifestations occur. Among the various molecular imaging techniques, this review mainly focuses on positron emission tomography (PET) imaging of atherosclerosis. The targets and pathways that have been investigated to date for PET imaging of atherosclerosis include: glycolysis, cell membrane metabolism (phosphatidylcholine synthesis), integrin $\alpha_3\beta_3$, low density lipoprotein (LDL) receptors (LDLR), natriuretic peptide clearance receptors (NPCRs), fatty acid synthesis, vascular cell adhesion molecule-1 (VCAM-1), macrophages, platelets, etc. Many PET tracers have been investigated clinically for imaging of atherosclerosis. Early diagnosis of atherosclerotic lesions by PET imaging can help to prevent the premature death caused by atherosclerosis, and smooth translation of promising PET tracers into the clinic is critical to the benefit of patients.

Key words: Positron emission tomography (PET), atherosclerosis, molecular imaging, vulnerable plaques, cardiovascular diseases.

Introduction

Atherosclerosis is a leading cause of death in developed countries and it is crucial to distinguish the unstable plaques from the stable ones to increase the survival of patients with early intervention [1]. The initial abnormality in the pathogenesis of atherosclerotic plaques is the fatty streak, a white/yellow linear discoloration that is visible macroscopically on the endothelial surface of an artery, caused by accumulation of lipids and macrophages. This initial lesion matures into an atherosclerotic plaque with the accumulation of lipid and connective tissue, in particular collagen. As the plaque grows, the vessel expands to preserve the blood flow, a process known as posi-

tive remodeling. The artery eventually can expand no farther, and the plaque begins to occlude the lumen of the vessel causing circulatory obstruction [2-4] (**Figure 1**). Unstable plaques that are prone to cardiovascular accidents demonstrate a thin fibrous cap, large lipid core, paucity of smooth muscle cells and abundance of inflammatory cells (**Figure 2**) [5, 6].

Clinical imaging of atherosclerosis

Traditionally atherosclerosis is visualized based on the anatomical changes in the vessel walls such as calcification and stenosis. Many techniques have been used for imaging of atherosclerosis in the clinic, such

as X-ray angiography, optical coherence tomography (OCT), intravascular ultrasound (US), computed tomography (CT), magnetic resonance imaging (MRI), single photon emission computed tomography (SPECT), positron emission tomography (PET), etc. [4]. Angiography yields an excellent resolution but it is highly observer dependent and not very reproducible [7-9]. Moreover diffuse arterial narrowing without obvious luminal irregularity can be easily missed in angiographic images [10]. Even if angiography could demonstrate the luminal narrowing accurately, it has been documented that acute coronary syndromes often result from plaque rupture at sites with no or only modest luminal narrowing based on angiography [11-13].

Molecular imaging of atherosclerosis

Many biological changes take place in atherosclerotic plaques preceding the appearance of anatomical disturbances [24, 25]. Given that a large proportion of people who suffer a sudden cardiac event have no prior symptoms [26], it is crucial for diagnostic procedures to go beyond the simple assessment of the vessel lumen to identify rupture-prone vulnerable

plaques [6]. When compared with traditional methods, molecular imaging approaches have a number of advantages, such as enabling noninvasive study of cells in their natural microenvironment hence providing information on the whole biological process rather than a small part of it. In terms of experimental studies it is possible to perform longitudinal studies in the same animals with molecular imaging techniques, which will reduce the cost and can provide better statistical power.

Since the beginning of the 21st century, the field of molecular imaging has expanded tremendously [27-34]. Many of the preclinical imaging studies focused on atherosclerosis involved the use of MRI and/or optical techniques, for which excellent recent reviews are available [4, 6, 11, 35-37]. A few other imaging techniques have also been employed for imaging of atherosclerosis such as Raman spectroscopy, which measures the light-scattering effects [23, 38]. In one study, Raman spectroscopy was used for imaging atherosclerosis associated inflammation with protease-activated fluorescent probes (representing capthesin-B and matrix metalloprotease (MMP)-2/9 expression) [39].

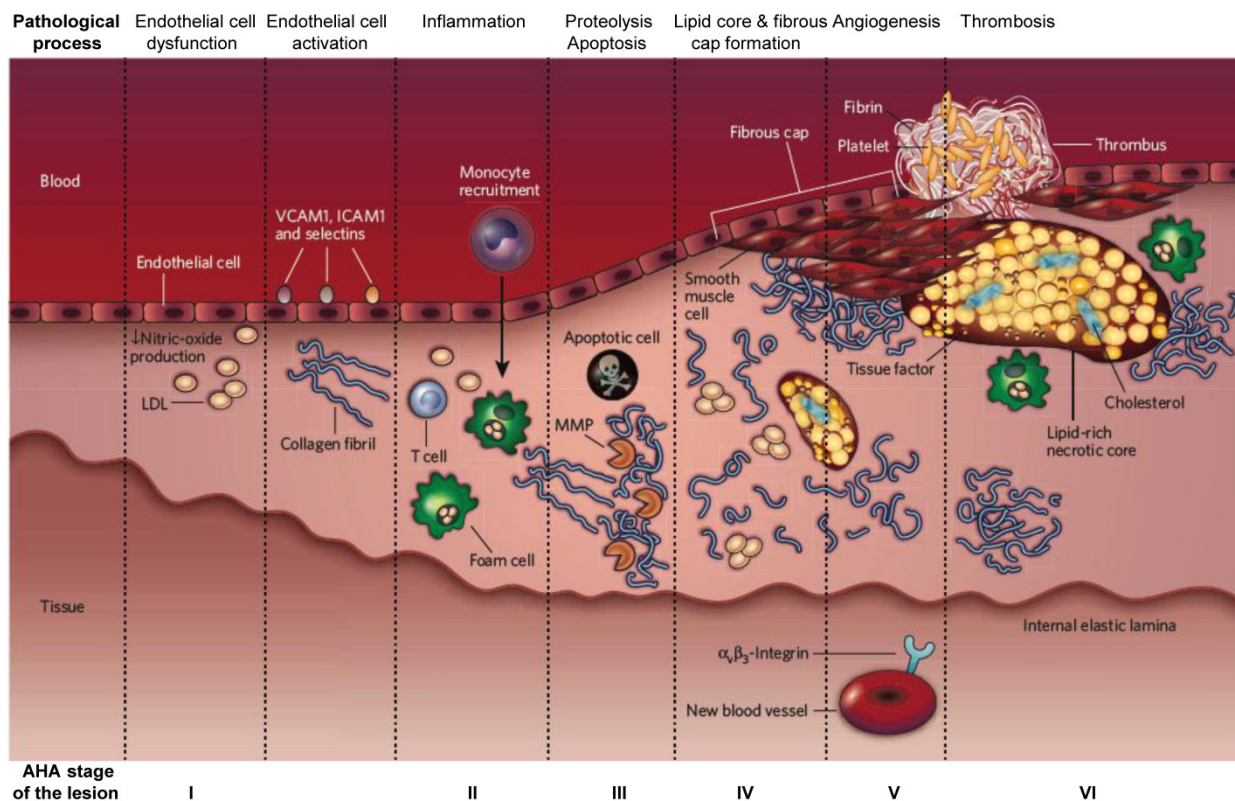


Fig 1. The developmental stages of an atherosclerotic lesion. AHA (American Heart Association) stage of the disease is indicated at the bottom of each corresponding column. Adapted from reference [6].

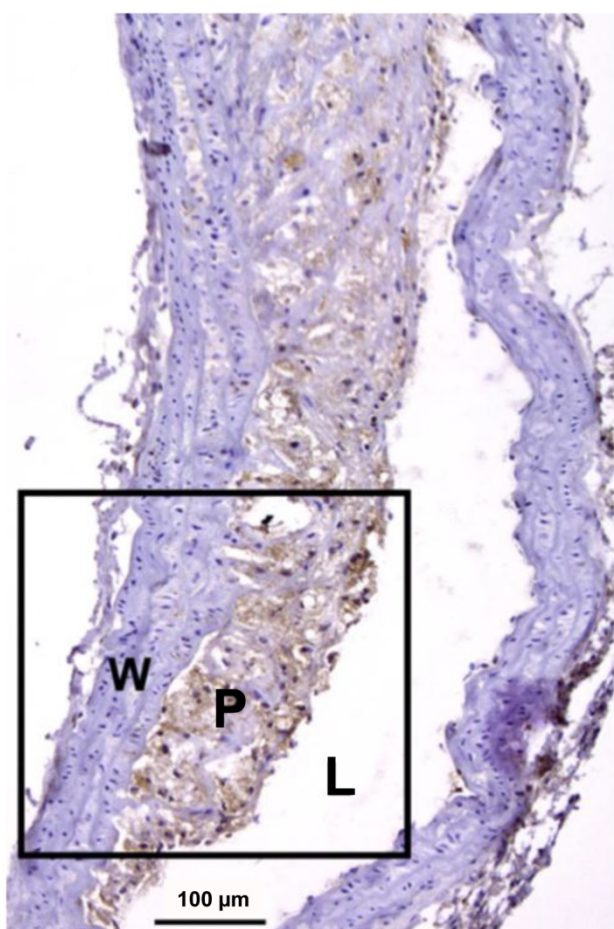


Fig 2. Mac-3 immunostaining of a severely inflamed atherosclerotic plaque. Macrophages are seen in brown, while adventitia and healthy vessel wall areas were Mac-3 negative. L: lumen; P: plaque; W: wall. Adapted from reference [79].

Molecular vascular imaging with PET can enable early detection of these changes, thereby decreasing the dependence to invasive biopsies or surgical procedures to characterize diseased tissues [11, 20, 23, 24, 40, 41]. PET can detect tracer concentrations in the picomolar range, providing 4-5 mm resolution with clinical PET scanners and 1-2 mm with small animal PET scanners, and has been routinely used in clinical cancer patient management and preclinical research [42-48]. Although there is no optimal PET tracer for routine clinical imaging of atherosclerosis available to date [10], various imaging agents have been investigated for PET imaging of atherosclerosis, targeting different components of the atherosclerotic plaque (Table 1).

In this review, we will summarize the targets and tracers used for PET imaging of atherosclerosis in experimental and clinical studies. The targets and pathways that have been investigated to date for PET imaging of atherosclerosis include: glycolysis, cell membrane metabolism (phosphatidylcholine synthesis), integrin $\alpha_v\beta_3$, low density lipoprotein (LDL) re-

ceptors (LDLr), natriuretic peptide clearance receptors (NPCRs), fatty acid synthesis, vascular cell adhesion molecule-1 (VCAM-1), macrophages, platelets, etc. (Table 1). To create experimental models for atherosclerosis, animals are typically kept on a high fat diet. Commonly used animal models for studying atherosclerosis are: C57BL/6 Apolipoprotein (Apo) E^{-/-} mice, C57BL/6 LDL receptor deficient mice (LDLr^{-/-} mice), heterozygous LDL receptor deficient rabbits (LDLr^{+/-} rabbits), and homozygous LDL receptor deficient rabbits (LDLr^{-/-} rabbits) [49-51]. The aorta is typically used as the human coronary artery analog in rodents since the diameter of mouse aorta is ~1 mm, comparable to the size of small arteries in humans [11].

Table 1. Summary of targets and tracers used for PET imaging of atherosclerosis.

Target	Tracer	Preclinical	Clinical
Glucose metabolism	¹⁸ F-FDG	[52, 53, 59]	[10, 54-58, 60, 63]
Membrane metabolism	¹⁸ F-choline	[65]	-
	¹¹ C-choline	-	[67]
Integrin $\alpha_v\beta_3$	¹⁸ F-galacto-RGD	[68]	[69]
LDLr	¹²⁴ I-CD68-Fc-ox-LDL	[70]	-
	¹⁸ F-nLDL & ox-LDL	[71]	-
NPCR	⁶⁴ Cu-DOTA-C-ANF	[72, 73]	-
Fatty acid synthesis	¹¹ C-acetate	-	[74]
VCAM-1	¹⁸ F-V4	[77]	-
Macrophages	⁶⁴ Cu-TNP	[78]	-
	⁶⁸ Ga	[79]	-
	¹¹ C-PK11195	-	[81]
Platelets	¹⁸ F-AppCHFppA	[82]	-

PET imaging of atherosclerosis with ¹⁸F-FDG

2-deoxy-2-¹⁸F-fluoro-D-glucose (¹⁸F-FDG) is one of the most frequently used PET tracers for in vivo imaging of atherosclerosis [4]. Deoxyglucose is a glucose analog that competes with glucose for uptake into metabolically active macrophages in atherosclerotic plaques. After being labeled with ¹⁸F, the resultant ¹⁸F-FDG is taken up into metabolically active cells but is not metabolized and thereby accumulates in atherosclerotic plaques (Figure 3A) [4]. More than 15 years ago, studies have demonstrated uptake of ¹⁸F-FDG in the region of the aortic arch in a rabbit model of atherosclerosis [52], while normal rabbits did not show increased uptake above background levels. Ex vivo analysis of the aortic arch confirmed ¹⁸F-FDG uptake in areas of atherosclerosis that were rich in macrophages. In another early study, Lederman et al. [53] documented a 4-fold increase in

^{18}F -FDG uptake by atherosclerotic plaques in iliac arteries of New Zealand White rabbits fed with high cholesterol diet.

A number of studies have been reported in patients. Yun et al. [10] reported the increased uptake of ^{18}F -FDG in 137 consecutive patients correlated with atherogenic risk factors. Among all risk factors, age was found to be the most significant factor. In another study, Rudd et al. [54] documented the ability of ^{18}F -FDG PET to image inflammation within carotid artery atherosclerotic plaques in 8 patients with symptomatic carotid atherosclerosis, who had experienced a recent carotid territory transient ischemic attack (TIA) and had an internal carotid artery stenosis of at least 70%. Several other clinical studies followed [55-58].

However, in a study carried out by Laurberg et al. [59], the authors did not observe increased aortic or carotid tracer accumulation in hypercholesterolemic, ApoE^{-/-} mice. Moreover, Menezes et al. [60] retro-

spectively examined 250 PET/CT images of 50 patients covering a 5 year period and found that they could not reproduce the similar results in subsequent images in patients with initially increased ^{18}F -FDG uptake in carotids and the aorta. Therefore, it was concluded that increased ^{18}F -FDG uptake in arterial lesions is a transient phenomenon. The discrepancy between the results of these studies and others remains unexplained [61, 62]. In an interesting report, it was shown that different mechanisms for stimulation of macrophages, smooth muscle cells, and endothelial cells may contribute to increased ^{18}F -FDG uptake in atherosclerotic plaques [63]. Experimental evidence suggested that hypoxia may play an important role in ^{18}F -FDG accumulation in atheromata, which deserves to be investigated in more detail in animal models and clinical settings to further our understanding of the biological mechanisms and significance of ^{18}F -FDG uptake in atheromata.

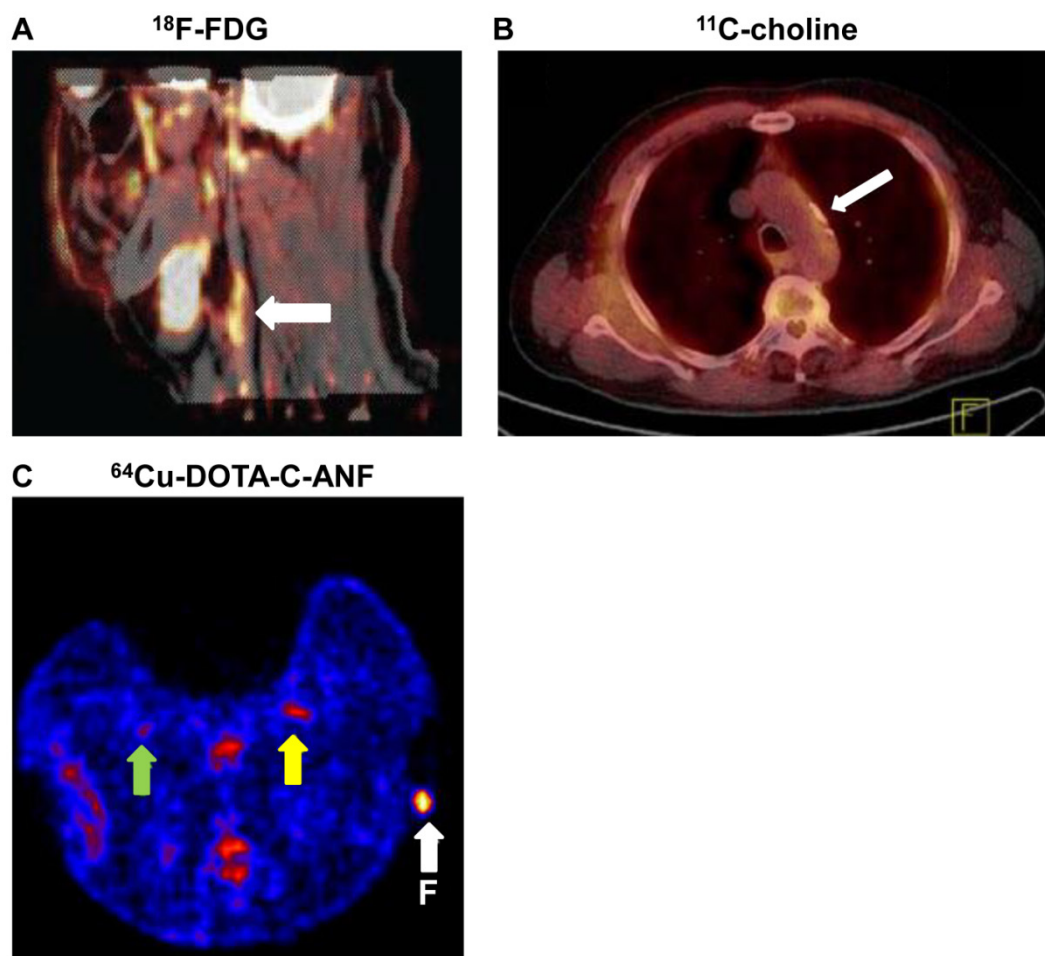


Fig 3. PET imaging of atherosclerosis with various tracers. **A.** Carotid atherosclerotic lesion in a male patient visualized by PET/CT. White arrows show ^{18}F -FDG uptake at the level of the plaque in carotid artery. **B.** ^{11}C -choline PET/CT images of the aortic arch of a male patient. White arrow indicates the atherosclerotic lesion. **C.** A representative transverse PET slice demonstrating the uptake of ^{64}Cu -DOTA-C-ANF on injured (yellow arrow) and control (green arrow) arteries in rabbit femoral artery. F (arrow): fiducial marker. Adapted from references [4, 67, 72].

PET imaging of atherosclerosis with radiolabeled choline

Choline is taken up into cells by specific transport mechanisms, phosphorylated by choline kinase, metabolized into phosphatidylcholine, and eventually incorporated into the cell membrane [61]. Increased uptake of choline has been observed in activated macrophages [64], which led to the idea of using radiolabeled choline for PET imaging of atherosclerotic plaques. For example, Matter et al. [65] used ^{18}F -Choline as the tracer to detect atherosclerotic plaques in ApoE $^{-/-}$ mice and reported superior results when compared with ^{18}F -FDG. Laitinen et al. [66] observed a high ^{11}C -choline uptake in the aortic plaques of atherosclerotic mice deficient for both LDLr and apolipoprotein B48. Kato et al. [67] reported an increased ^{11}C -choline uptake in vessel walls of 93 consecutive male patients between 60 and 80 years old (**Figure 3B**). However, PET tracer uptake and calcification are rarely co-localized. Therefore, it was concluded that ^{11}C -choline has the potential to provide information about atherosclerotic plaques independent of calcification measurement.

PET imaging of atherosclerosis targeting integrin $\alpha_v\beta_3$

Integrin $\alpha_v\beta_3$ is a cell adhesion molecule expressed by macrophages and endothelial cells in atherosclerotic lesions [4]. Laitinen et al. [68] evaluated integrin $\alpha_v\beta_3$ deposition in atherosclerotic plaques in mice with ^{18}F -galacto-RGD PET (RGD denotes arginine-glycine-aspartic acid, potent antagonists of integrin $\alpha_v\beta_3$). They dissected the aorta of mice 2 hours after tracer injection and found that biodistribution of ^{18}F -galacto-RGD was higher in the atherosclerotic than in the normal aorta, and ^{18}F -galacto-RGD uptake was directly correlated with macrophage density in the plaques. In a previous clinical study, Beer et al. [69] investigated the dosimetry of ^{18}F -galacto-RGD in 18 human subjects and concluded that it demonstrates high metabolic stability, a favorable biodistribution, and a low radiation dose. Therefore, this tracer can safely be used for noninvasive PET imaging of molecular processes (e.g. atherosclerosis) involving integrin $\alpha_v\beta_3$.

PET imaging of atherosclerosis with ^{18}F -labeled LDL

Oxidation of LDL is regarded as a crucial event in atherogenesis. Langer et al. [70] conjugated ^{124}I to the scavenger receptor CD68 (soluble CD68-Fc) and used this molecule for the detection of atherosclerotic plaques in wild type or ApoE $^{-/-}$ mice. Since CD68

binds to oxidized LDL (ox-LDL) molecules and mediates their uptake, this tracer could be a useful tool for noninvasive imaging of atherosclerosis. In another study, Pietzsch et al. [71] reported PET imaging with ^{18}F -labeled native LDL (nLDL) and ox-LDL after injection into male Wistar rats. It was suggested that the use of ^{18}F -labeled LDL could be an attractive alternative to iodinated LDL. Future studies are warranted to clarify the potential of radiolabeled LDL for the detection of atherosclerotic changes.

PET imaging of atherosclerosis targeting NPCR

Natriuretic peptides (NPs) have potent antiproliferative and antimigratory effects on vascular smooth-muscle cells and participate in vascular remodeling in atherosclerosis. The expression of NPCRs is upregulated both in endothelium and in vascular smooth-muscle cells during the formation of atherosclerotic plaques [72]. Liu et al. [72] investigated the potential of radiolabeled C-type atrial natriuretic factor (C-ANF) to noninvasively image developing plaque-like lesions. C-ANF was linked with 1,4,7,10-tetraazacyclododecane-1,4,7,10-tetraacetic acid (DOTA) and labeled with ^{64}Cu for noninvasive PET in a hypercholesterolemic rabbit model, which demonstrated that ^{64}Cu -DOTA-C-ANF was a promising candidate for PET of NPCR in atherosclerotic plaques (**Figure 3C**). In a follow-up study, the same group developed a C-ANF-integrated, ^{64}Cu -labeled nanoprobe for in vivo PET imaging of NPCR during angiogenesis in a mouse hindlimb ischemia model [73].

PET imaging of atherosclerosis with other tracers

In addition to the abovementioned examples, many other tracers have been investigated for imaging of atherosclerosis. Derlin et al. [74] used ^{11}C -acetate PET/CT for the evaluation of atherosclerotic plaques in 36 patients (**Figure 4**). Fatty acids are a common constituent of atherosclerotic plaque and may be synthesized in the plaque itself. Fatty acid synthesis requires acetyl-coenzyme-A (CoA) as a main substrate, which is produced from acetate. Therefore, ^{11}C -acetate, just like ^{18}F -FDG, can be used as a non-specific tracer for in vivo imaging of atherosclerotic plaques.

VCAM-1 is a monocyte and lymphocyte adhesion factor expressed by endothelial cells under pro-atherogenic conditions [75, 76]. Nahrendorf et al. [77] have investigated the potential of VCAM-1 as a target for PET imaging of vulnerable plaques. A tetrameric VCAM-1 affinity peptide (V4), which can be

internalized into endothelial cells after VCAM-1 binding, was labeled with ^{18}F and tested in atherosclerotic ApoE $^{-/-}$ mice receiving a high-cholesterol diet. The tracer was found to be suitable for noninvasive PET imaging of VCAM-1 in inflammatory atherosclerosis, as well as monitoring the effects of therapeutic intervention. In another study, Nahrendorf et al. [78] also reported the use of a ^{64}Cu -labeled, dextranated, diethylenetriaminepentaacetic acid (DTPA)-modified magnetofluorescent nanoparticle for imaging of atherosclerotic plaques. The agent was termed ^{64}Cu -TNP (i.e. trireporter nanoparticle), where its uptake in atherosclerosis was based on the avidity of lesional macrophages for polysaccharide-containing supramolecular structures. It was found that ^{64}Cu -TNP accumulated predominantly in macrophages in atherosclerotic plaques in ApoE $^{-/-}$ mice (Figure 5).

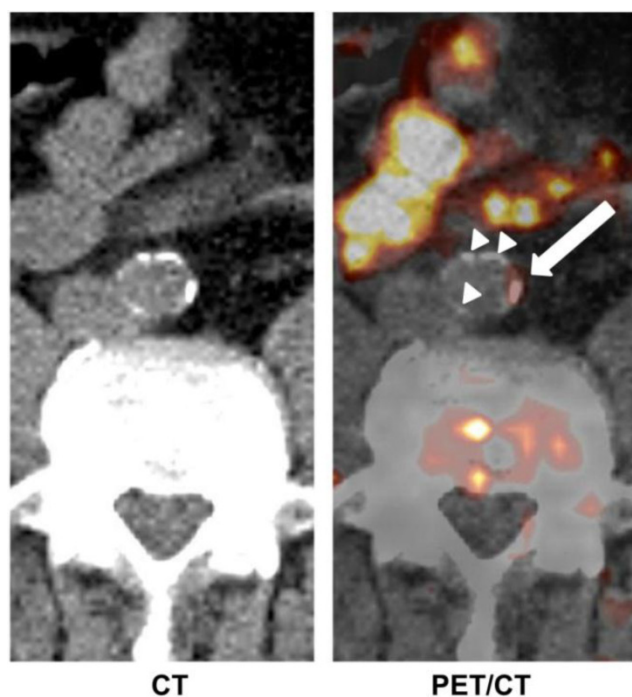


Fig 4. Transaxial ^{11}C -acetate PET/CT images of abdominal aorta of a male patient. Tracer uptake in vessel wall coincided with calcification in some areas (white arrow), whereas other calcifications of comparable size did not accumulate ^{11}C -acetate (white arrow heads). Adapted from reference [74].

Silvola et al. [79] investigated the uptake of ionic ^{68}Ga in atherosclerotic LDLr $^{-/-}$ /ApoB100/100 mice. PET/CT imaging revealed an elevated ^{68}Ga uptake in the aortic atherosclerotic plaques of mice, especially at the sites that are rich in macrophages. Ex vivo biodistribution studies and autoradiography of aortic cryosections confirmed the results of in vivo imaging. However, it was stated that the slow blood clearance may limit the clinical usability of ^{68}Ga as a PET tracer

for imaging of atherosclerosis. In another study, Yano et al. [80] suggested that ^{68}Ga -labeled platelets could be useful for PET imaging of thrombosis or atherosclerosis. However, no in vivo studies were carried out, although in vitro labeling of rabbit platelets with ^{68}Ga was successful.

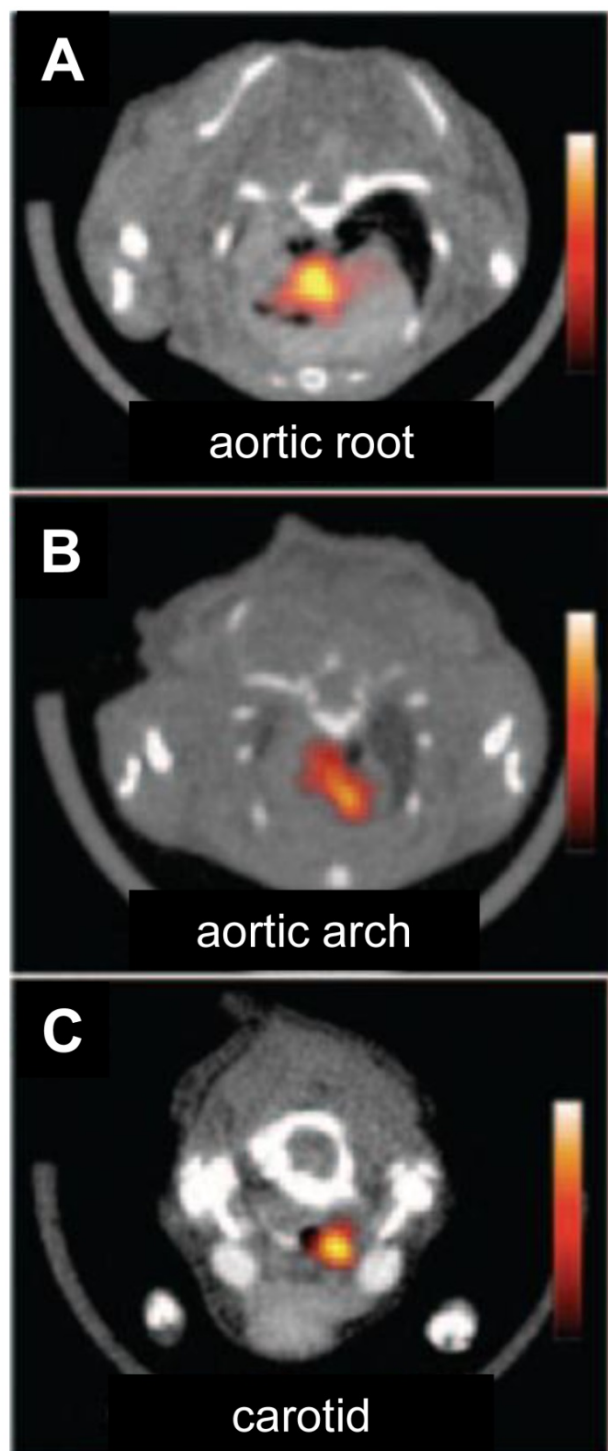


Fig 5. PET/CT imaging of inflammatory atherosclerosis in ApoE $^{-/-}$ mice injected with ^{64}Cu -TNP. Adapted from reference [78].

Gaemperli et al. [81] recently suggested the use of ^{11}C -PK11195, a selective ligand of the translocator protein which is highly expressed by activated macrophages, for PET imaging of atherosclerosis. Initial results obtained from 32 patients with carotid stenosis were encouraging. Elmaleh et al. [82] evaluated PET imaging with ^{18}F -AppCHFppA, a competitive inhibitor of adenosine diphosphate-induced platelet aggregation, to detect atherosclerotic lesions in male New Zealand White rabbits. It was reported that the accumulation of ^{18}F -AppCHFppA in macrophage rich atherosclerotic plaques could be quantified noninvasively.

Conclusion and future perspectives

A wide variety of targets and tracers have been investigated for PET imaging of atherosclerosis, which has significant potential for translation and future clinical imaging of atherosclerosis. Among these PET tracers, inflammation-targeted tracers seem particularly promising. Monocytes, macrophages, and foam cells play important roles in the evolution and complications of atherosclerosis [83]. Following their migration to the lesion site, these cells scavenge lipids, secrete cytokines that further amplify inflammation and produce proteases that can be noninvasively visualized with the use of suitable tracers [11, 83]. The most commonly used PET tracer for imaging of atherosclerosis is ^{18}F -FDG, with many other tracers already tested clinically: ^{11}C -choline [67], ^{18}F -galacto-RGD [69], ^{11}C -acetate [74], and ^{11}C -PK11195 [81]. Since ^{11}C -PK11195 specifically binds to macrophages through translocator proteins that are highly expressed on activated macrophages, it may provide more specificity for imaging of atherosclerosis than ^{18}F -FDG.

An important contribution of PET imaging of atherosclerosis will be to determine the at-risk individuals earlier in the disease process by targeting one of the abovementioned components at the early stage of disease. It may also prove to be useful in determining the biological responses to certain therapeutic intervention. The key strengths of PET include its excellent sensitivity, limitless depth of penetration, and quantitation capabilities [27]. However, the small size of the atherosclerotic lesions and their vicinity with blood, the unbound/circulating tracer activity, and the continuous respiratory and cardiac movements during the acquisition of the images are the unsolved issues in PET imaging of atherosclerosis [11, 12, 84]. The availability of PET/MR systems [85, 86], where MRI can provide high spatial resolution and exquisite soft tissue contrast to complement PET, may dramatically facilitate the translation of promising PET tracers into the clinic for atherosclerosis imaging.

Measurement of regional and global calcification of the heart and major arteries using ^{18}F -NaF PET/CT may also be useful for early detection of atherosclerosis [87]. This technique may provide highly relevant information about the state of calcified plaque before structural calcification is detectable by standard CT techniques, thereby allowing for earlier intervention for risk reduction in cardiovascular diseases [87, 88]. Another potential target for the PET imaging of atherosclerosis is CD105 (i.e. endoglin), where it was demonstrated that precursor atherosclerotic lesions exhibit intimal neovascularization that are associated with increased CD105 expression on endothelial cells [89-91]. In addition, CD105 also plays a role in restenosis after stent placement [92], therefore can be used as a marker for the progression of coronary atherosclerosis. We have recently developed a series of CD105-targeted PET and/or optical imaging probes [93-96], which may be applied for PET imaging of atherosclerosis in the near future. In conclusion, PET imaging of atherosclerosis is still at a nascent stage which needs significant future research effort. Smooth clinical translation of promising PET tracers into the clinic is critical to the benefit of patients.

Acknowledgment

This work is supported, in part, by the University of Wisconsin - Madison, the National Institutes of Health (NIBIB/NCI 1R01CA169365), the Department of Defense (W81XWH-11-1-0644), and the American Cancer Society (125246-RSG-13-099-01-CCE).

Competing Interests

The authors have declared that no competing interest exists.

References

- Falk E, Shah PK, Fuster V. Coronary plaque disruption. *Circulation*. 1995; 92: 657-71.
- Davignon J, Ganz P. Role of endothelial dysfunction in atherosclerosis. *Circulation*. 2004; 109: III27-32.
- Falk E. Pathogenesis of atherosclerosis. *J Am Coll Cardiol*. 2006; 47: C7-12.
- Davies JR, Rudd JH, Weissberg PL. Molecular and metabolic imaging of atherosclerosis. *J Nucl Med*. 2004; 45: 1898-907.
- Davies MJ. Stability and instability: two faces of coronary atherosclerosis. The Paul Dudley White Lecture 1995. *Circulation*. 1996; 94: 2013-20.
- Wu JC, Bengel FM, Gambhir SS. Cardiovascular molecular imaging. *Radiology*. 2007; 244: 337-55.
- Galbraith JE, Murphy ML, de Soyza N. Coronary angiogram interpretation. Interobserver variability. *JAMA*. 1978; 240: 2053-6.
- Leape LL, Park RE, Bashore TM, Harrison JK, Davidson CJ, Brook RH. Effect of variability in the interpretation of coronary angiograms on the appropriateness of use of coronary revascularization procedures. *Am Heart J*. 2000; 139: 106-13.
- Nissen SE, Yock P. Intravascular ultrasound: novel pathophysiological insights and current clinical applications. *Circulation*. 2001; 103: 604-16.
- Yun M, Jang S, Cucchiara A, Newberg AB, Alavi A. ^{18}F FDG uptake in the large arteries: a correlation study with the atherogenic risk factors. *Semin Nucl Med*. 2002; 32: 70-6.
- Leuschner F, Nahrendorf M. Molecular imaging of coronary atherosclerosis and myocardial infarction: considerations for the bench and perspectives for the clinic. *Circ Res*. 2011; 108: 593-606.
- Lucignani G, Schafers M. PET, CT and MRI characterisation of the atherosclerotic plaque. *Eur J Nucl Med Mol Imaging*. 2010; 37: 2398-402.

13. Fuster V, Badimon L, Badimon JJ, Chesebro JH. The pathogenesis of coronary artery disease and the acute coronary syndromes (1). *N Engl J Med*. 1992; 326: 242-50.
14. Yucel EK, Anderson CM, Edelman RR, Grist TM, Baum RA, Manning WJ, et al. AHA scientific statement. Magnetic resonance angiography : update on applications for extracranial arteries. *Circulation*. 1999; 100: 2284-301.
15. Tearney GJ, Yabushita H, Houser SL, Aretz HT, Jang IK, Schlendorf KH, et al. Quantification of macrophage content in atherosclerotic plaques by optical coherence tomography. *Circulation*. 2003; 107: 113-9.
16. Raggi P. Coronary calcium on electron beam tomography imaging as a surrogate marker of coronary artery disease. *Am J Cardiol*. 2001; 87: 27A-34A.
17. Peterson TE, Manning HC. Molecular imaging: ¹⁸F-FDG PET and a whole lot more. *J Nucl Med Technol*. 2009; 37: 151-61.
18. Wong ST. Emerging treatment combinations: integrating therapy into clinical practice. *Am J Health Syst Pharm*. 2009; 66: S9-S14.
19. Massoud TF, Gambhir SS. Integrating noninvasive molecular imaging into molecular medicine: an evolving paradigm. *Trends Mol Med*. 2007; 13: 183-91.
20. Schillaci O, Danieli R, Padovano F, Testa A, Simonetti G. Molecular imaging of atherosclerotic plaque with nuclear medicine techniques. *Int J Mol Med*. 2008; 22: 3-7.
21. Erbel R, Ge J, Bockisch A, Kearney P, Gorge G, Haude M, et al. Value of intracoronary ultrasound and Doppler in the differentiation of angiographically normal coronary arteries: a prospective study in patients with angina pectoris. *Eur Heart J*. 1996; 17: 880-9.
22. Deshpande N, Needles A, Willmann JK. Molecular ultrasound imaging: current status and future directions. *Clin Radiol*. 2010; 65: 567-81.
23. Pysz MA, Gambhir SS, Willmann JK. Molecular imaging: current status and emerging strategies. *Clin Radiol*. 2010; 65: 500-16.
24. Cavalcanti Filho JL, de Souza Leao Lima R, de Souza Machado Neto L, Kayat Bittencourt L, Domingues RC, da Fonseca LM. PET/CT and vascular disease: current concepts. *Eur J Radiol*. 2011; 80: 60-7.
25. Yoshinaga K, Manabe O, Tamaki N. Assessment of coronary endothelial function using PET. *J Nucl Cardiol*. 2011; 18: 486-500.
26. Myerburg RJ, Interian A, Jr., Mitrani RM, Kessler KM, Castellanos A. Frequency of sudden cardiac death and profiles of risk. *Am J Cardiol*. 1997; 80: 10F-9F.
27. James ML, Gambhir SS. A molecular imaging primer: modalities, imaging agents, and applications. *Physiol Rev*. 2012; 92: 897-965.
28. Bhargava P, He G, Samarghandi A, Delpassand ES. Pictorial review of SPECT/CT imaging applications in clinical nuclear medicine. *Am J Nucl Med Mol Imaging*. 2012; 2: 221-31.
29. Cai W, Zhang Y, Kamp TJ. Imaging of induced pluripotent stem cells: from cellular reprogramming to transplantation. *Am J Nucl Med Mol Imaging*. 2011; 1: 18-28.
30. Huang X, Lee S, Chen X. Design of "smart" probes for optical imaging of apoptosis. *Am J Nucl Med Mol Imaging*. 2011; 1: 3-17.
31. Thorek DLJ, Robertson R, Bacchus WA, Hahn J, Rothberg J, Beattie BJ, et al. Cerenkov imaging - a new modality for molecular imaging. *Am J Nucl Med Mol Imaging*. 2012; 2: 163-73.
32. Yigit MV, Medarova Z. In vivo and ex vivo applications of gold nanoparticles for biomedical SERS imaging. *Am J Nucl Med Mol Imaging*. 2012; 2: 232-41.
33. Zeman MN, Scott PJH. Current imaging strategies in rheumatoid arthritis. *Am J Nucl Med Mol Imaging*. 2012; 2: 174-220.
34. Zhang Y, Cai W. Molecular imaging of insulin-like growth factor 1 receptor in cancer. *Am J Nucl Med Mol Imaging*. 2012; 2: 248-59.
35. Owen DR, Lindsay AC, Choudhury RP, Fayad ZA. Imaging of atherosclerosis. *Annu Rev Med*. 2011; 62: 25-40.
36. Glaudemans AW, Slart RH, Bozzao A, Bonanno E, Arca M, Dierckx RA, et al. Molecular imaging in atherosclerosis. *Eur J Nucl Med Mol Imaging*. 2010; 37: 2381-97.
37. Sadeghi MM, Glover DK, Lanza GM, Fayad ZA, Johnson LL. Imaging atherosclerosis and vulnerable plaque. *J Nucl Med*. 2010; 51 Suppl 1: 51S-65S.
38. Motz JT, Fitzmaurice M, Miller A, Gandhi SJ, Haka AS, Galindo LH, et al. In vivo Raman spectral pathology of human atherosclerosis and vulnerable plaque. *J Biomed Opt*. 2006; 11: 021003.
39. Kim DE, Kim JY, Schellingerhout D, Kim EJ, Kim HK, Lee S, et al. Protease imaging of human atheromata captures molecular information of atherosclerosis, complementing anatomic imaging. *Arterioscler Thromb Vasc Biol*. 2010; 30: 449-56.
40. Mankoff DA. A definition of molecular imaging. *J Nucl Med*. 2007; 48: 18N, 21N.
41. Hoffman JM, Gambhir SS. Molecular imaging: the vision and opportunity for radiology in the future. *Radiology*. 2007; 244: 39-47.
42. Alauddin MM. Positron emission tomography (PET) imaging with ¹⁸F-based radiotracers. *Am J Nucl Med Mol Imaging*. 2012; 2: 55-76.
43. Cai W, Hong H. Peptoid and positron emission tomography: an appealing combination. *Am J Nucl Med Mol Imaging*. 2011; 1: 76-9.
44. De Saint-Hubert M, Brepoels L, Devos E, Vermaelen P, De Groot T, Tousseyn T, et al. Molecular imaging of therapy response with ¹⁸F-FLT and ¹⁸F-FDG following cyclophosphamide and mTOR inhibition. *Am J Nucl Med Mol Imaging*. 2012; 2: 110-21.
45. Eary JF, Hawkins DS, Rodler ET, Conrad EUL. ¹⁸F-FDG PET in sarcoma treatment response imaging. *Am J Nucl Med Mol Imaging*. 2011; 1: 47-53.
46. Grassi I, Nanni C, Allegrì V, Morigi JJ, Montini GC, Castellucci P, et al. The clinical use of PET with ¹¹C-acetate. *Am J Nucl Med Mol Imaging*. 2012; 2: 33-47.
47. Iagaru A. ¹⁸F-FDG PET/CT: timing for evaluation of response to therapy remains a clinical challenge. *Am J Nucl Med Mol Imaging*. 2011; 1: 63-4.
48. Vach W, Høilund-Carlson PF, Fischer BM, Gerke O, Weber W. How to study optimal timing of PET/CT for monitoring of cancer treatment. *Am J Nucl Med Mol Imaging*. 2011; 1: 54-62.
49. Chakrabarti M, Cheng KT, Spicer KM, Kirsch WM, Fowler SD, Kelln W, et al. Biodistribution and radioimmunopharmacokinetics of ¹³¹I-Ama monoclonal antibody in atherosclerotic rabbits. *Nucl Med Biol*. 1995; 22: 693-7.
50. Calcagno C, Cornily JC, Hyafil F, Rudd JH, Briley-Saebo KC, Mani V, et al. Detection of neovessels in atherosclerotic plaques of rabbits using dynamic contrast enhanced MRI and ¹⁸F-FDG PET. *Arterioscler Thromb Vasc Biol*. 2008; 28: 1311-7.
51. Van Craeyveld E, Gordts SC, Singh N, Jacobs F, De Geest B. A critical reassessment of murine and rabbit models of atherosclerosis: focus on lesion progression and remodelling. *Acta Cardiol*. 2012; 67: 11-21.
52. Vallabajosula S MK, Knesaurek J. Imaging atherosclerotic macrophage density by positron emission tomography using F-18-fluorodeoxyglucose (FDG) [abstract]. *J Nucl Med Technol*. 1996; 37(suppl): 38P.
53. Lederman RJ, Raylman RR, Fisher SJ, Kison PV, San H, Nabel EG, et al. Detection of atherosclerosis using a novel positron-sensitive probe and 18-fluorodeoxyglucose (FDG). *Nucl Med Commun*. 2001; 22: 747-53.
54. Rudd JH, Warburton EA, Fryer TD, Jones HA, Clark JC, Antoun N, et al. Imaging atherosclerotic plaque inflammation with [¹⁸F]-fluorodeoxyglucose positron emission tomography. *Circulation*. 2002; 105: 2708-11.
55. Wykrzykowska J, Lehman S, Williams G, Parker JA, Palmer MR, Varkey S, et al. Imaging of inflamed and vulnerable plaque in coronary arteries with ¹⁸F-FDG PET/CT in patients with suppression of myocardial uptake using low-carbohydrate, high-fat preparation. *J Nucl Med*. 2009; 50: 563-8.
56. Bural CG, Torigan DA, Chamroonrat W, Houseni M, Chen W, Basu S, et al. FDG-PET is an effective imaging modality to detect and quantify age-related atherosclerosis in large arteries. *Eur J Nucl Med Mol Imaging*. 2008; 35: 562-9.
57. Alexanderson E, Slomka P, Cheng V, Meave A, Saldana Y, Garcia-Rojas L, et al. Fusion of positron emission tomography and coronary computed tomographic angiography identifies plaque 18 fluorodeoxyglucose uptake in the left main coronary artery soft plaque. *J Nucl Cardiol*. 2008; 15: 841-3.
58. Li Y, Berenji GR, Shaba WF, Tafti B, Yevdayev E, Dadparvar S. Association of vascular fluoride uptake with vascular calcification and coronary artery disease. *Nucl Med Commun*. 2012; 33: 14-20.
59. Laurberg JM, Olsen AK, Hansen SB, Bottcher M, Morrison M, Ricketts SA, et al. Imaging of vulnerable atherosclerotic plaques with FDG-microPET: no FDG accumulation. *Atherosclerosis*. 2007; 192: 275-82.
60. Menezes LJ, Kayani I, Ben-Haim S, Hutton B, Ell PJ, Groves AM. What is the natural history of ¹⁸F-FDG uptake in arterial atheroma on PET/CT? Implications for imaging the vulnerable plaque. *Atherosclerosis*. 2010; 211: 136-40.
61. Riou LM, Broisat A, Dimastromatteo J, Pons G, Fagret D, Ghezzi C. Pre-clinical and clinical evaluation of nuclear tracers for the molecular imaging of vulnerable atherosclerosis: an overview. *Curr Med Chem*. 2009; 16: 1499-511.
62. Rudd JH, Fayad ZA, Machac J, Weissberg PL, Davies JR, Warburton EA, et al. Response to 'Laurberg JM, Olsen AK, Hansen SB, et al. Imaging of vulnerable atherosclerotic plaques with FDG-microPET: no FDG accumulation' [Atherosclerosis 2006]. *Atherosclerosis*. 2007; 192: 453-4; author reply 1-2.
63. Folco EJ, Sheikine Y, Rocha VZ, Christen T, Shvartz E, Sukhova GK, et al. Hypoxia but not inflammation augments glucose uptake in human macrophages: Implications for imaging atherosclerosis with ¹⁸fluorine-labeled 2-deoxy-D-glucose positron emission tomography. *J Am Coll Cardiol*. 2011; 58: 603-14.
64. Boggs KP, Rock CO, Jackowski S. Lysophosphatidylcholine and 1-O-octadecyl-2-O-methyl-rac-glycero-3-phosphocholine inhibit the CDP-choline pathway of phosphatidylcholine synthesis at the CTP:phosphocholine cytidyltransferase step. *J Biol Chem*. 1995; 270: 7757-64.
65. Matter CM, Wyss MT, Meier P, Spahn N, von Lukowicz T, Lohmann C, et al. ¹⁸F-choline images murine atherosclerotic plaques ex vivo. *Arterioscler Thromb Vasc Biol*. 2006; 26: 584-9.
66. Laitinen IE, Luoto P, Nagren K, Marjamaki PM, Silvola JM, Hellberg S, et al. Uptake of ¹¹C-choline in mouse atherosclerotic plaques. *J Nucl Med*. 2010; 51: 798-802.
67. Kato K, Schober O, Ikeda M, Schafers M, Ishigaki T, Kies P, et al. Evaluation and comparison of ¹¹C-choline uptake and calcification in aortic and common carotid arterial walls with combined PET/CT. *Eur J Nucl Med Mol Imaging*. 2009; 36: 1622-8.
68. Laitinen I, Saraste A, Weidl E, Poethko T, Weber AW, Nekolla SG, et al. Evaluation of alphavbeta3 integrin-targeted positron emission tomography tracer ¹⁸F-galacto-RGD for imaging of vascular inflammation in atherosclerotic mice. *Circ Cardiovasc Imaging*. 2009; 2: 331-8.
69. Beer AJ, Haubner R, Wolf I, Goebel M, Luderschmidt S, Niemeyer M, et al. PET-based human dosimetry of ¹⁸F-galacto-RGD, a new radiotracer for imaging alpha v beta3 expression. *J Nucl Med*. 2006; 47: 763-9.
70. Langer HF, Haubner R, Pichler BJ, Gawaz M. Radionuclide imaging: a molecular key to the atherosclerotic plaque. *J Am Coll Cardiol*. 2008; 52: 1-12.
71. Pietzsch J, Bergmann R, Wuest F, Pawelke B, Hultsch C, van den Hoff J. Catabolism of native and oxidized low density lipoproteins: in vivo insights

- from small animal positron emission tomography studies. *Amino Acids*. 2005; 29: 389-404.
72. Liu Y, Abendschein D, Woodard GE, Rossin R, McCommis K, Zheng J, et al. Molecular imaging of atherosclerotic plaque with (64)Cu-labeled natriuretic peptide and PET. *J Nucl Med*. 2010; 51: 85-91.
73. Liu Y, Pressly ED, Abendschein DR, Hawker CJ, Woodard GE, Woodard PK, et al. Targeting angiogenesis using a C-type atrial natriuretic factor-conjugated nanoprobe and PET. *J Nucl Med*. 2011; 52: 1956-63.
74. Derlin T, Habermann CR, Lengyel Z, Busch JD, Wisotzki C, Mester J, et al. Feasibility of ¹¹C-acetate PET/CT for imaging of fatty acid synthesis in the atherosclerotic vessel wall. *J Nucl Med*. 2011; 52: 1848-54.
75. Kinlay S, Libby P, Ganz P. Endothelial function and coronary artery disease. *Curr Opin Lipidol*. 2001; 12: 383-9.
76. Ley K, Huo Y. VCAM-1 is critical in atherosclerosis. *J Clin Invest*. 2001; 107: 1209-10.
77. Nahrendorf M, Keliher E, Panizzi P, Zhang H, Hembrador S, Figueiredo JL, et al. ¹⁸F-4V for PET-CT imaging of VCAM-1 expression in atherosclerosis. *JACC Cardiovasc Imaging*. 2009; 2: 1213-22.
78. Nahrendorf M, Zhang H, Hembrador S, Panizzi P, Sosnovik DE, Aikawa E, et al. Nanoparticle PET-CT imaging of macrophages in inflammatory atherosclerosis. *Circulation*. 2008; 117: 379-87.
79. Silvola JM, Laitinen I, Sipila HJ, Laine VJ, Leppanen P, Yla-Herttuala S, et al. Uptake of ⁶⁸Ga in atherosclerotic plaques in LDLR-/-ApoB100/100 mice. *EJNMMI Res*. 2011; 1: 14.
80. Yano Y, Budinger TF, Ebbe SN, Mathis CA, Singh M, Brennan KM, et al. Gallium-68 lipophilic complexes for labeling platelets. *J Nucl Med*. 1985; 26: 1429-37.
81. Gaemperli O, Shalhoub J, Owen DR, Lamare F, Johansson S, Fouladi N, et al. Imaging intraplaque inflammation in carotid atherosclerosis with ¹¹C-PK11195 positron emission tomography/computed tomography. *Eur Heart J*. 2012; 33:1902-10.
82. Elmaleh DR, Fischman AJ, Tawakol A, Zhu A, Shoup TM, Hoffmann U, et al. Detection of inflamed atherosclerotic lesions with diadenosine-5',5'''-P1,P4-tetraphosphate (Ap4A) and positron-emission tomography. *Proc Natl Acad Sci U S A*. 2006; 103: 15992-6.
83. Libby P. Inflammation in atherosclerosis. *Nature*. 2002; 420: 868-74.
84. Wang Y, Vidan E, Bergman GW. Cardiac motion of coronary arteries: variability in the rest period and implications for coronary MR angiography. *Radiology*. 1999; 213: 751-8.
85. Loeffelbein DJ, Souvatzoglou M, Wankerl V, Martinez-Moller A, Dinges J, Schwaiger M, et al. PET-MRI fusion in head-and-neck oncology: current status and implications for hybrid PET/MRI. *J Oral Maxillofac Surg*. 2012; 70: 473-83.
86. Zaidi H, Del Guerra A. An outlook on future design of hybrid PET/MRI systems. *Med Phys*. 2011; 38: 5667-89.
87. Beheshti M, Saboury B, Mehta NN, Torigian DA, Werner T, Mohler E, et al. Detection and global quantification of cardiovascular molecular calcification by fluoro18-fluoride positron emission tomography/computed tomography--a novel concept. *Hell J Nucl Med*. 2011; 14: 114-20.
88. Basu S, Hoiland-Carlson PF, Alavi A. Assessing global cardiovascular molecular calcification with ¹⁸F-fluoride PET/CT: will this become a clinical reality and a challenge to CT calcification scoring? *Eur J Nucl Med Mol Imaging*. 2012; 39: 660-4.
89. Piao M, Tokunaga O. Significant expression of endoglin (CD105), TGFbeta-1 and TGFbeta R-2 in the atherosclerotic aorta: an immunohistological study. *J Atheroscler Thromb*. 2006; 13: 82-9.
90. Luque A, Turu M, Juan-Babot O, Cardona P, Font A, Carvajal A, et al. Overexpression of hypoxia/inflammatory markers in atherosclerotic carotid plaques. *Front Biosci*. 2008; 13: 6483-90.
91. Luque A, Slevin M, Turu MM, Juan-Babot O, Badimon L, Krupinski J. CD105 positive neovessels are prevalent in early stage carotid lesions, and correlate with the grade in more advanced carotid and coronary plaques. *J Angiogenesis Res*. 2009; 1: 6.
92. Pelliccia F, Cianfrocca C, Rosano G, Mercurio G, Speciale G, Pasceri V. Role of endothelial progenitor cells in restenosis and progression of coronary atherosclerosis after percutaneous coronary intervention: a prospective study. *JACC Cardiovasc Interv*. 2010; 3: 78-86.
93. Zhang Y, Hong H, Engle JW, Yang Y, Theuer CP, Barnhart TE, et al. Positron emission tomography and optical imaging of tumor CD105 expression with a dual-labeled monoclonal antibody. *Mol Pharm*. 2012; 9: 645-53.
94. Zhang Y, Hong H, Engle JW, Bean J, Yang Y, Leigh BR, et al. Positron emission tomography imaging of CD105 expression with a ⁶⁴Cu-labeled monoclonal antibody: NOTA is superior to DOTA. *PLoS One*. 2011; 6: e28005.
95. Hong H, Severin GW, Yang Y, Engle JW, Zhang Y, Barnhart TE, et al. Positron emission tomography imaging of CD105 expression with ⁸⁹Zr-Df-TRC105. *Eur J Nucl Med Mol Imaging*. 2012; 39: 138-48.
96. Hong H, Yang Y, Zhang Y, Engle JW, Barnhart TE, Nickles RJ, et al. Positron emission tomography imaging of CD105 expression during tumor angiogenesis. *Eur J Nucl Med Mol Imaging*. 2011; 38: 1335-43.